The relativity of color perception

Michel Berthier, Valérie Garcin, Nicoletta Prencipe, Edoardo Provenzi

The relativity of color perception

Michel Berthier*[1], Valérie Garcin†[2], Nicoletta Prencipe‡[3] and Edoardo Provenzi§[4]

[1]Laboratoire MIA, Pôle Sciences et Technologie, Université de La Rochelle, Avenue Michel Crépeau, 17042 La Rochelle Cedex 1
[2,3,4]Université de Bordeaux, CNRS, Bordeaux INP, IMB, UMR 5251, F-33400, 351 Cours de la Libération, Talence, France

Abstract

Inspired by the pioneering work of H. Yilmaz, we propose in this paper a mathematical formalization of the relativistic nature of color perception that relies on a single axiom: the space of perceived colors is the positive cone of a three dimensional formally real Jordan algebra. If this Jordan algebra is taken to be the spin factor $\mathbb{R} \oplus \mathbb{R}^2$, then we get a natural description of a perceived color as a real positive magnitude, which encodes an information related to luminance, together with a chromatic vector, that carries an information related to hue and saturation. We show that chromatic vectors follow the relativistic addition rule, which turns out to be equivalent with the use of the Hilbert metric to measure chromatic differences. This metric is shown to be compatible with experimental data. Up to authors' knowledge, this work proofs that color perception is the first relativistic phenomenon not related to movement ever discovered in nature.

1 Introduction

In 1962, H. Yilmaz proposed in [5] a description of color perception that shown analogies with Einstein's special theory of relativity. Although very original and ahead of his time, Yilmaz's analysis was based on quite questionable experimental results. In this paper, we prove that a relativistic theory of color perception can be developed in a well-defined mathematical context, without the necessity to resort to any empirical data.

Our working framework is based on a single assumption, called *trichromacy axiom*, in which perceived colors are assumed to be elements of the positive cone of a formally real Jordan algebra of dimension 3. Thanks to the classification of such algebras, the only non-trivial one satisfying the trichromacy axiom is the spin factor $\mathbb{R} \oplus \mathbb{R}^2$, or its naturally isomorphic counterpart represented by $\mathcal{H}(2, \mathbb{R})$, the Jordan algebra of 2×2 real symmetric matrices.

The interplay between these Jordan algebras has major consequences for our theory. On one side, the positive cone of $\mathcal{H}(2, \mathbb{R})$ contains density matrices that reveal a hidden link between color perception and algebraic quantum theories. On the other side, the positive cone of $\mathbb{R} \oplus \mathbb{R}^2$ allows us to describe perceived colors through positive real magnitudes α together with chromatic vectors $\mathbf{v}$ satisfying the relativistic addition rule. Moreover, we prove that the Hilbert metric is the only perceptual color distance compatible with the relativistic behavior of chromatic vectors.

The structure of the paper is as follows: in section 1, after a brief historical introduction, we introduce a suitable mathematical framework for the formalization of Yilmaz's results (quoted in the appendix), describing its assets and drawbacks. In section 2 we introduce the quantum setting

*michel.berthier@univ-lr.fr
†valerie.garcin@math.u-bordeaux.fr
‡nicoletta.prencipe@math.u-bordeaux.fr
§edoardo.provenzi@math.u-bordeaux.fr

for the study of color perception and Hering's opponency. We start section 3 by introducing a novel nomenclature and we use it to set up the proof of the relativistic behavior of chromatic vectors, which turns out to single out the Hilbert metric to measure chromatic differences. We end section 3 by showing that this metric is compatible with experimental data. Finally, in section 4, we show how to interpret the third, most puzzling, result of Yilmaz's experiments in terms of relativistic aberration and boost maps. Conclusions and perspectives future works will end the paper.

1.1 On color perception

The first noticeable mathematical contribution on color perception dates back to Newton and his celebrated 1704 book "Opticks" [1]. Newton noticed that the set of perceived colors has the structure of a *cone*, which has been proven to be *convex* and embedded in a linear space of dimension 3 (for trichromatic vision) by Grassmann one century and a half later [2]. In the same years, Riemann pointed out, in his famous 1854 Habilitation lecture [3] that the only simple examples of abstract manifolds that one can practically encounter are those of positions of perceived objects and colors. Finally, in 1920, Schrödinger [4] recasted the previous findings on color perception in a coherent set of axioms that can be resumed in a modern language by saying that *the space of perceived colors has the structure of a regular convex cone of dimension 3*. Schrödinger also emphazised the importance of the 'infinitesimal line element' to compute color differences.

In the same years, the recently formed International Commission on Illumination, or CIE, for "Commission Internationale de l'Éclairage", concerned by the expanding industrial needs, started a more pragmatically and less mathematically rigorous approach to model color perception. This marked a significant bifurcation with respect to the analysis of Schrödinger and his predecessors and eventually led to the organisation of perceived colors into empirical spaces with several ad-hoc parameters, whose validity is limited to very restrictive conditions, almost never verified by natural visual scenes. The influence of CIE on color spaces has been so pervasive that we have to wait until 1962 to find a significant alternative to CIE recommendations. To the best of our knowledge, Yilmaz's paper [5] seems to be the first, and the only contribution that investigates the geometry of color perception from the point of view of relativity. The main aim of its author was to obtain *colorimetric Lorentz transformations* by interpreting mathematically the results of three basic experiments.

1.2 Yilmaz experiments

In order to analyse the results of *color matching experiments*, Yilmaz considers the following space:

$$\mathcal{C} = \{(\alpha, x, y) \in \mathbb{R}^3,\ \Sigma^2 - \|\mathbf{v}\|^2 \geq 0,\ \alpha \geq 0\}\ , \tag{1}$$

where $\mathbf{v} = (v_1, v_2) = (x/\alpha, y/\alpha)$ with $\alpha > 0$; if $\alpha = 0$, then also $\mathbf{v}$ is null. A color[1] c of $\mathcal{C}$ can be viewed both as a point of $\mathbb{R}^3$ with coordinates (α, x, y) and as a couple $(\alpha, \mathbf{v})$, where α is a positive real number and $\mathbf{v}$ is a vector of $\mathbb{R}^2$ of Euclidean norm $v = \|\mathbf{v}\|$ less or equal to Σ. The norm v is the *saturation* of the color c, the angle defined by $\phi = \arctan(y/x)$ its *hue*, and the positive real α its *lightness*. The existence of a positive real Σ, which plays the role of a *limiting saturation* 'reached by spectral colors', is one of the fundamental assumptions of Yilmaz.

Notice that the definition of saturation given above is the analogue of speed (the magnitude of the velocity vector) in mechanics, thus it seems coherent to interpret the limiting saturation Σ as an analogue of the light speed.

Roughly speaking, the purpose of the three experiments described in [5] is to show that:

1. color perception is a relativistic phenomenon;

2. the limiting saturation is constant under 'illuminant changes';

[1] To avoid all possible misleading interpretation, we underline that, throughout the whole paper, we use the word *color* to mean a *perceived color*.

3. there exists a colorimetric aberration effect which is the analogue of the relativistic one.

It is worth mentioning that Yilmaz does not use any information related to a hypothetical invariant quadratic form. The goal of the third experiment is precisely to bypass the introduction of an invariant metric whose existence is very difficult to justify experimentally.

In order to strengthen and formalize the analogy between color perception and relativity, setting up a suitable nomenclature and notation is an essential step. For this reason, we introduce here some complementary definitions borrowed from mechanics and adapted to our framework.

Without any further specification, we consider a color c as an abstract *coordinate-free* element of the space $\mathcal{C}$. This interpretation is the exact analogue to what we do in Galileian mechanics when we consider the position as an abstract element of the space $\mathbb{R}^3$ without coordinates.

A coordinate system can be introduced on $\mathcal{C}$ by considering an illuminant[2] which allows us to identify c and to perform measurements on it, for this reason, here we define an *illuminant* to be *a reference frame I of the space $\mathcal{C}$*. It is well-known, see e.g. [21, 18], that when an observer is embedded for a sufficient time in a visual scene illuminated by I, he/she will perceive the surface of an object characterized by non-selective reflectance properties without a color saturation. In this case, we call that observer *adapted* to I. This consideration naturally leads us to call any couple $o = (c, I)$, such that the color $c \in \mathcal{C}$ has zero saturation in the reference frame I, an observer adapted to an illuminant I, or simply an *observer* from now on. Given the analogy between the saturation of a color and the speed of a velocity vector for a mechanical system, an observer $o = (c, I)$ is characterized by the fact that the color c appears 'at rest' in the reference frame I.

Carrying on the analogy with mechanics, we will call $o_1 = (c_1, I_1)$ and $o_2 = (c_2, I_2)$ two *inertial observers*. Given $i, j = 1, 2$, c_j will be described by o_i with a color $c_j^i = (\alpha, \mathbf{v}_{ij})$, for a certain vector $\mathbf{v}_{ij}$ such that $\|\mathbf{v}_{ij}\| \leq \Sigma$ and, by definition of observer, $c_i^i = (\alpha, \mathbf{0})$, being c_i^i the coordinate representation of c_i w.r.t. I_i, $i = 1, 2$.

Given two inertial observers o_1 and o_2, we denote by (α^1, x^1, y^1) the coordinates of the reference frame I_1 and by (α^2, x^2, y^2) the coordinates of the reference frame I_2.

We refer to [5], or to the appendix, for the description of the three experiments under discussion, in which Yilmaz considers only the case of one non zero component of the $\mathbf{v}$ vector: $\mathbf{v}_{c_1} = (v_{c_1}, 0)$, $\mathbf{v}_{c_2} = (v_{c_2}, 0)$, and $\mathbf{v}_{12} = (v_{12}, 0)$.

The result of the first experiment can be expressed mathematically by the following equalities:

$$\mathbf{v}_{c_2^1} = \mathbf{v}_{12}, \quad \mathbf{v}_{c_1^2} = -\mathbf{v}_{12} \ . \tag{2}$$

Since, for $i, j = 1, 2$, $i \neq j$, the saturation of c_i is null in the reference frame I_i and different from zero in the reference frame j, eq. (2) clearly shows that *color perception is a relativistic phenomenon*.

Also the second experiment involves two inertial observers $o_1 = (c_1, I_1)$ and $o_2 = (c_2, I_2)$, both describing the same color c. The result of the second experiment can be summarized as follows:

$$\mathbf{v}_{c^1} = (\Sigma, 0) \Longrightarrow \mathbf{v}_{c^2} = (\Sigma, 0) \ , \tag{3}$$

i.e., *colors with limiting saturation are perceived as such by all inertial observers*.

As already mentioned, the third experiment is meant to mimic the relativistic aberration effect. Once again, it involves two inertial observers o_1 and o_2, both observing the same color c, different from the previous one. The result of the third experiment is the following:

$$\mathbf{v}_{c^1} = (0, \Sigma) \Longrightarrow \mathbf{v}_{c^2} = (-\Sigma \sin\varphi, \Sigma \cos\varphi) \ , \tag{4}$$

with $\sin\varphi = v_{12}/\Sigma$. As we will see, this experiment is crucial for the derivation of the colorimetric Lorentz transformations.

[2]More precisely, we should call it a broadband illuminant, i.e. a light source extended over the entire visible spectrum. The reason is that, if we consider a narrow-band illuminant, the so-called Helson-Judd effect enters into play and an observer will experience an *incomplete adaptation*, see e.g. [21]. For the sake of simplicity, we will implicitly consider *an illuminant as broadband without further specifications*.

1.3 Derivation of colorimetric Lorentz transformations

We explain now how to obtain the colorimetric Lorentz transformations from eqs. (2), (3) and (4). In [5] the coordinate change between o_1 and o_2 is supposed to be linear. It is easy to check that taking into account the specific choices made by Yilmaz, the coordinate change is given by:

$$\begin{pmatrix} \alpha^2 \\ x^2 \\ y^2 \end{pmatrix} = \begin{pmatrix} a_{11} & a_{12} & 0 \\ a_{21} & a_{22} & 0 \\ 0 & 0 & 1 \end{pmatrix} \begin{pmatrix} \alpha^1 \\ x^1 \\ y^1 \end{pmatrix} \ . \tag{5}$$

Consequently, we have:

$$\frac{x_2}{\alpha_2} = \frac{a_{21}\alpha_1 + a_{22}x_1}{a_{11}\alpha_1 + a_{12}x_1}, \quad \frac{x_1}{\alpha_1} = \frac{-a_{21}\alpha_2 + a_{11}x_2}{a_{22}\alpha_2 - a_{12}x_2} \ . \tag{6}$$

The two equalities of eq. (2) are equivalent to:

$$\frac{a_{21}}{a_{11}} = -v_{12}, \quad \frac{-a_{21}}{a_{22}} = v_{12} \ . \tag{7}$$

This shows that: $a_{11} = a_{22}$ and $a_{21} = -v_{12}a_{22}$.

The result of the second experiment, eq. (3), is equivalent to:

$$\Sigma = \frac{a_{21} + a_{22}\Sigma}{a_{11} + a_{12}\Sigma} \ , \tag{8}$$

which gives: $a_{12} = -(v_{12}a_{22})/\Sigma^2$.

From the third experiment, eq. (4), we have:

$$-\tan\varphi = \frac{a_{21}\alpha_1 + a_{22}x_1}{y_1} = \frac{a_{21}}{\Sigma} \ . \tag{9}$$

Since $\sin\varphi = v_{12}/\Sigma$, this implies:

$$a_{22} = \frac{1}{\sqrt{1 - (v_{12}/\Sigma)^2}} \ . \tag{10}$$

Finally:

$$\begin{pmatrix} \alpha^2 \\ x^2 \\ y^2 \end{pmatrix} = \begin{pmatrix} \frac{1}{\sqrt{1-(v_{12}/\Sigma)^2}} & \frac{-v_{12}/\Sigma^2}{\sqrt{1-(v_{12}/\Sigma)^2}} & 0 \\ \frac{-v_{12}}{\sqrt{1-(v_{12}/\Sigma)^2}} & \frac{1}{\sqrt{1-(v_{12}/\Sigma)^2}} & 0 \\ 0 & 0 & 1 \end{pmatrix} \begin{pmatrix} \alpha^1 \\ x^1 \\ y^1 \end{pmatrix} \ . \tag{11}$$

It is worth noticing that the derivation of these colorimetric Lorentz transformations proposed by Yilmaz relies only on information given by the **v**-component of colors[3], the only one appearing in eqs. (2), (3) and (4).

1.4 Towards a relativistic theory of color perception

Without calling into question the great originality of Yilmaz's ideas and the relevance of his results, we deem necessary to underline some issues about the approach that we have reported above. As mentioned before, the derivation of the colorimetric Lorentz transformations is essentially based on the following assumptions:

1. the space of *perceived colors* is the cone $\mathcal{C}$, and, in particular, there exists a limiting saturation Σ;

2. the coordinate changes between inertial observers are linear transformations;

[3] In the sequel we will emphasize the crucial role of these *chromatic vectors*.

3. the results obtained from the three experiments are considered as valid.

However, no experimental result, nor apparatus description is available in [5] and this naturally raises doubts about the actual implementation of the three experiments. Furthermore, while the results of first two seem convincing, the outcome of the third seems completely illusory. In fact, Yilmaz defines the limiting saturation of a color $c = (\alpha, \mathbf{v}) \in \mathcal{C}$ as a value Σ of $\|v\|$ that cannot be perceptually matched with that of any Munsell chip, thus, while this definition permits to *identify* the limiting saturation of a color, it does not allow its *measurement*. As a consequence, eq. (4), with its precise analytical form, seems to be an ad-hoc formula used to single out the colorimetric Lorentz transformations (11), more than the real outcome of a psycho-physical experiment.

It may be tempting to adopt a more conventional approach to obtain the desired transformations starting, for instance, from the fact that there exists a limiting saturation invariant under observer changes and that the color space is isotropic and homogeneous. But to go further, it is necessary to introduce an analogue of the Minkowski metric, which Yilmaz precisely circumvents. One may choose to follow the standard path used in special relativity, see e.g. [19, 20], to justify the existence of such a metric. However, while the assumptions that go along with this approach rely on a solid experimental basis for what concerns the Minkowski spacetime, they are far from being either obvious or simple to be tested for the space of perceived colors. For this reason, we consider a better solution to follow less conventional, but fully equivalent, approaches to special relativity as, e.g., that of the remarkable Mermin's paper [6], whose main focus is the Einstein-Poincaré velocity addition law and not the Lorentz transformations. This alternative path can be considered as a mathematical analogue of Yilmaz's experimental approach to the relativity of color perception and it is in this sense that we consider the present work to be a formalization of his groundbreaking ideas ahead of his time.

1.5 Outline of the paper

Section 2 is devoted to the geometric structure of the space of perceived colors. We resume the main results of [7] and [8]. The only assumption we make is formulated in the form of a *trichromacy axiom* which is based on the axioms of Schrödinger. We recall, for instance, how to recover the color opponency from a quantum point of view. In section 3 we explain how to obtain Einstein-Poincaré addition law for *chromatic vectors* in a very simple and natural way. This allows, in particular, to justify that the relevant metric on the space of chromatic vectors is the Hilbert metric, which is proven to be confirmed by psychovisual measurement data reported in [16] and [17]. We show in section 4 how *chromatic states* generate one-parameter subgroups of Lorentz boosts. By studying the action of these boosts of the space of chromatic vectors we recover the colorimetric aberration effect from the sole trichromacy axiom.

2 The space of perceived colors

This section is devoted to recall some basic information about the geometry of the space of perceived colors. We refer to [7], [8] and [9] for more details and references, especially for a description of the seminal work of Resnikoff [10].

2.1 The thrichromacy cone

We are going to introduce our only axiom for the space of perceived colors. The path that leads to this axiom can be succinctly summarized as follows. The classical, and well established, colorimetric experiences of Newton, Grassmann and Helmholtz have been resumed by Schrödinger in a set of axioms that can be mathematically translated by stating that the space of perceived colors by a standard trichromatic observer is a regular convex cone of real dimension 3. In [10], Resnikoff analyzed the consequences of the hypothesis of homogeneity, i.e. of the existence of a transitive group action, on this space. He also had the remarkable idea of recasting this assumption in the setting of Jordan algebras, but he did not fully exploit the powerful results available from

the general theory of these algebras. This was done by Berthier in [7] and the result is the following axiom.

TRICHROMACY AXIOM [7]: – *The space of perceived colors is the positive cone*[4] *of a formally real Jordan algebra of real dimension 3.*

It can be shown that such a Jordan algebra is isomorphic either to the sum $\mathbb{R} \oplus \mathbb{R} \oplus \mathbb{R}$ or to the Jordan algebra $\mathcal{H}(2, \mathbb{R})$ of 2 by 2 symmetric matrices with real entries [11]. The positive cone of the former is the product $\mathbb{R}^+ \times \mathbb{R}^+ \times \mathbb{R}^+$. When equipped with the so-called Helmhotz-Stiles metric:

$$ds^2 = \sum_{i=1}^{3} a_i \left(d\xi_i/\xi_i\right)^2 \ , \tag{12}$$

$a_i, \xi_i \in \mathbb{R}^+$, it is the metric space used in standard colorimetry. Since this space has been extensively studied, in the sequel we will concentrate only on the second possibility which, as we will see, has a much richer structure.

A crucial remark is that $\mathcal{H}(2, \mathbb{R})$ is isomorphic, as a Jordan algebra, to the *spin factor* $\mathbb{R} \oplus \mathbb{R}^2$ whose Jordan product is defined by:

$$(\alpha_1 + \mathbf{v}_1) \circ (\alpha_2 + \mathbf{v}_2) = (\alpha_1\alpha_2 + \langle \mathbf{v}_1, \mathbf{v}_2 \rangle + \alpha_1\mathbf{v}_2 + \alpha_2\mathbf{v}_1) \ , \tag{13}$$

where α_1 and α_2 are reals, $\mathbf{v}_1$ and $\mathbf{v}_2$ are vectors of $\mathbb{R}^2$ and $\langle \ , \ \rangle$ denotes the Euclidean scalar product on $\mathbb{R}^2$. An explicit isomorphism of Jordan algebras is given by:

$$\chi : (\alpha + \mathbf{v}) \in \mathbb{R} \oplus \mathbb{R}^2 \longmapsto \begin{pmatrix} \alpha + v_1 & v_2 \\ v_2 & \alpha - v_1 \end{pmatrix} \in \mathcal{H}(2, \mathbb{R}) \ , \tag{14}$$

where $\mathbf{v} = (v_1, v_2)$.

The positive cone of the Jordan algebra $\mathcal{H}(2, \mathbb{R})$ is the set of positive semi-definite 2 by 2 symmetric matrices with real entries. Via the isomorphism χ it corresponds to the positive cone of the spin factor $\mathbb{R} \oplus \mathbb{R}^2$. This latter is given by:

$$\mathcal{C} = \{(\alpha + \mathbf{v}) \in \mathbb{R} \oplus \mathbb{R}^2, \ \alpha^2 - \|\mathbf{v}\|^2 \geq 0, \ \alpha \geq 0\} \ . \tag{15}$$

In the following, $\mathcal{C}$ is called the *trichromacy cone*. Notice that the trichromacy cone defined above differs from the cone introduced in (1) by the fact that $\mathbb{R} \oplus \mathbb{R}^2$ is endowed with a Jordan algebra structure.

2.2 Trichromacy and quantum color opponency

$\mathcal{H}(2, \mathbb{R})$ is the algebra of observables of the real analogue of a qubit called a *rebit*. The states of this quantum system are characterized by *density matrices*, i.e. positive elements of $\mathcal{H}(2, \mathbb{R})$ with trace equal to 1. It is clear that a matrix of $\mathcal{H}(2, \mathbb{R})$ written as in eq. (14) is a density matrix if and only if $\mathbf{v} = (v_1, v_2) \in \mathcal{D} = \{v \in \mathbb{R}^2, \ \|v\| \leq 1\}$ and $\alpha = 1/2$. Two explicit expressions for the density matrices are:

$$\rho(\mathbf{v}) = \frac{1}{2} \begin{pmatrix} 1 + v_1 & v_2 \\ v_2 & 1 - v_1 \end{pmatrix} \ , \tag{16}$$

and

$$\rho(\mathbf{v}) = \frac{1}{2}(Id_2 + \mathbf{v} \cdot \sigma) = \frac{1}{2}(Id_2 + v_1\sigma_1 + v_2\sigma_2) \ , \tag{17}$$

where Id_2 is the 2×2 identity matrix and $\sigma = (\sigma_1, \sigma_2)$, with:

$$\sigma_1 = \begin{pmatrix} 1 & 0 \\ 0 & -1 \end{pmatrix} \quad \sigma_2 = \begin{pmatrix} 0 & 1 \\ 1 & 0 \end{pmatrix} \ . \tag{18}$$

[4]The positive cone of a formally real Jordan algebra $\mathcal{A}$ is the set of squares of $\mathcal{A}$. According to the Koecher-Vinberg theorem [11], this axiom is equivalent to requiring that the interior of the space of perceived colors to be a symmetric cone of real dimension 3. Indeed, the trichromacy axiom differs from those of Schrödinger only by the fact that a symmetric cone is self dual and homogeneous.

If we consider the state vectors written in Dirac's notation as the following set of 'ket':

$$|u_1\rangle = \begin{pmatrix} 1 \\ 0 \end{pmatrix} \quad |d_1\rangle = \begin{pmatrix} 0 \\ 1 \end{pmatrix} \quad |u_2\rangle = \frac{1}{\sqrt{2}} \begin{pmatrix} 1 \\ 1 \end{pmatrix} \quad |d_2\rangle = \frac{1}{\sqrt{2}} \begin{pmatrix} -1 \\ 1 \end{pmatrix} , \tag{19}$$

then, by denoting with $\langle\ |\ =\ |\ \rangle^t$ the corresponding set of 'bra', we have:

$$\sigma_1 = |u_1\rangle\langle u_1| - |d_1\rangle\langle d_1| \quad \text{and} \quad \sigma_2 = |u_2\rangle\langle u_2| - |d_2\rangle\langle d_2| . \tag{20}$$

This shows that the state vectors $|u_1\rangle$ and $|d_1\rangle$, resp. $|u_2\rangle$ and $|d_2\rangle$, are eigenstates of σ_1, resp. σ_2, with eigenvalues 1 and -1.

The two matrices σ_1 and σ_2 are Pauli-like matrices that give a two direction opponency mechanism. More precisely, representing (v_1, v_2) in polar coordinates (r, θ), with $r \in [0, 1]$ and $\theta \in [0, 2\pi)$, the density matrix $\rho(\mathbf{v})$ can be written in three equivalent forms:

$$\rho(r, \theta) = \frac{1}{2} \begin{pmatrix} 1 + r\cos\theta & r\sin\theta \\ r\sin\theta & 1 - r\cos\theta \end{pmatrix} , \tag{21}$$

or:

$$\begin{aligned} \rho(r, \theta) = \frac{1}{2} \big(&(1 + r\cos\theta)|u_1\rangle\langle u_1| + (1 - r\cos\theta)|d_1\rangle\langle d_1| \\ &+(r\sin\theta)|u_2\rangle\langle u_2| \ -(r\sin\theta)|d_2\rangle\langle d_2| \big) , \end{aligned} \tag{22}$$

or, by noticing that $\sigma_1 = \rho(1, 0) - \rho(1, \pi)$ and $\sigma_2 = \rho(1, \pi/2) - \rho(1, 3\pi/2)$ and using eq. (17):

$$\rho(r, \theta) = \rho_0 + \frac{r\cos\theta}{2}(\rho(1, 0) - \rho(1, \pi)) + \frac{r\sin\theta}{2}(\rho(1, \pi/2) - \rho(1, 3\pi/2)) , \tag{23}$$

where $\rho_0 = Id_2/2$ and $\rho(r, \theta) = \rho_0$ if and only if $r = 0$. A useful representation of the rebit states is provided by the *Bloch disk*, see Fig. 2.2.

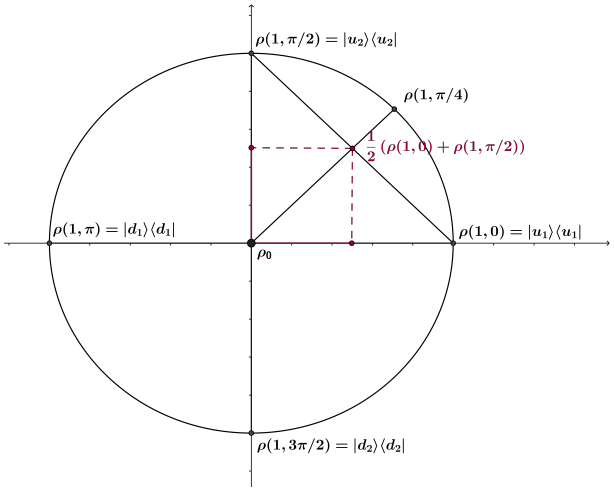

Figure 1: The Bloch disk of the rebit illustrating the opponency mechanism. The density matrix $\rho(1, \pi/4)$ is given by: $\rho(1, \pi/4) = |1, \pi/4\rangle\langle 1, \pi/4| = (|u_1\rangle + |u_2\rangle)(\langle u_1| + \langle u_2|)/(2 + \sqrt{2})$. The mixture $(\rho(1, 0) + \rho(1, \pi/2))/2$ is the density matrix: $\rho(\sqrt{2}/2, \pi/4) = \rho_0 + \frac{1}{4}(\rho(1, 0) - \rho(1, \pi)) + \frac{1}{4}(\rho(1, \pi/2) - \rho(1, 3\pi/2))$.

The density matrices parameterized by $r = 1$, independently on $\theta \in [0, 2\pi)$, i.e. $\rho(1, \theta)$, correspond to *pure states*. They are characterized by either the equation:

$$\rho(1, \theta) \circ \rho(1, \theta) = \rho(1, \theta) , \tag{24}$$

or, recalling that the von Neumann entropy of a generic density matrix ρ is defined as $-\text{Trace}(\rho \log \rho)$, by:

$$-\text{Trace}(\rho(1,\theta)\log\rho(1,\theta)) = 0 \ , \tag{25}$$

which means that their von Neumann entropy is zero. These pure state density matrices are the projector matrices:

$$\rho(1,\theta) = |1,\theta\rangle\langle 1,\theta| \ , \tag{26}$$

with $|1,\theta\rangle = \cos(\theta/2)|u_1\rangle + \sin(\theta/2)|d_1\rangle$. The density matrix ρ_0 that corresponds to the *state of maximal Von Neumann entropy* is $\rho_0 = Id_2/2$ and it can be written as the mixture:

$$\rho_0 = \frac{1}{4}\rho(1,0) + \frac{1}{4}\rho(1,\pi) + \frac{1}{4}\rho(1,\pi/2) + \frac{1}{4}\rho(1,3\pi/2) \ . \tag{27}$$

Eq. (23) shows that every density matrix is the sum of the state of maximal entropy with two other components that describe the opponency with respect to the two directions $(\rho(1,0),\rho(1,\pi))$ and $(\rho(1,\pi/2),\rho(1,3\pi/2))$. Given a density matrix $\rho(r,\theta)$, one can evaluate the contribution of the opposition $(\rho(1,0),\rho(1,\pi))$ given by σ_1 by computing:

$$\langle\sigma_1\rangle_{\rho(r,\theta)} = \text{Trace}(\rho(r,\theta)\circ\sigma_1) = r\cos\theta \ , \tag{28}$$

and the same for the other direction. It is quite remarkable that the Block disk of Fig. 2.2 gives a quantum analogue of the *Hering disk* that describes the color opponency mechanism resulting from the activity of certain retinal neurons [12]. The matrix σ_1 encodes the opposition red/green, while the matrix σ_2 encodes the opposition yellow/blue. We underline that this quantum justification of the color opponency derives only from the trichromacy axiom when considering the algebra $\mathcal{H}(2,\mathbb{R})$.

2.3 Colorimetric definitions

We introduce now some definitions that are used in the sequel. A *perceived color* c is an element of the trichromacy cone $\mathcal{C}$: $c = (\alpha + \mathbf{v})$ with $\alpha^2 - \|\mathbf{v}\|^2 \geq 0$ and $\alpha \geq 0$. The positive real α is called the *magnitude*[5] of c.

The case when c has magnitude $\alpha = 1/2$ is special, in fact, as previously seen, thanks to the isomorphism defined in eq. (14), c can naturally be associated to a density matrix representing its state. For this reason, in the sequel, a color with magnitude $1/2$ will be called a *color state*. To emphasize that a perceived color c is a color state we add the subscript s, so that the symbol c_s will denote a color $(1/2 + \mathbf{v})$, with $\|\mathbf{v}\| \leq 1/2$.

We can associate to any other color c with arbitrary magnitude $\alpha \geq 0$ a density matrix by considering the projection obtained by dividing c with respect to twice its first component, i.e. $c/2\alpha = (1/2 + \mathbf{v}/2\alpha)$, which belongs to $\mathcal{D}_{1/2} = \{c \in \mathcal{C},\ \alpha = 1/2\}$, the set of all perceived colors whose magnitude is fixed to $1/2$.

The vector $\mathbf{v}_c \in \mathcal{D}_{1/2}$ is called the *chromatic vector* of the color c because it carries only information about the chromatic attributes of c and not about its magnitude.

By using eq. (16), we can associate a density matrix to every chromatic vector $\mathbf{v}_c = (v_{c,1}, v_{c,2}) \in \mathcal{D}_{1/2}$ simply by considering $2\mathbf{v}_c \in \mathcal{D}$, which allows us to write:

$$\rho(2\mathbf{v}_c) = \frac{1}{2}\begin{pmatrix} 1+2v_{c,1} & 2v_{c,2} \\ 2v_{c,2} & 1-2v_{c,1} \end{pmatrix} \ . \tag{29}$$

For every perceived color $c \in \mathcal{C}$, the density matrix $\rho(2\mathbf{v}_c)$ characterizes the *chromatic state* of c. The difference between a color and a chromatic state is represented by the fact that, in the first case, the density matrix associated to a color c with magnitude $1/2$ contains all the information about the state of c, magnitude included, which is not the case for a chromatic state, where the magnitude α of c does not play any role.

[5] We prefer not to use the term *lightness* because of possible confusion. See for instance [13] for a discussion on the meaning of this word.

Two noticeable conditions about chromatic states can be singled out: the first is when the density matrix $\rho(2\mathbf{v}_c)$ describes a pure chromatic state, in this case, $c \in \mathcal{C}$ is said to be a *pure perceived color*. This condition is equivalent to $\|\mathbf{v}_c\| = 1/2$, so that pure perceived colors are in one-to-one correspondence with the points of the perimeter of the disk $\mathcal{D}_{1/2}$. The second noticeable condition is when $\rho(2\mathbf{v}_c)$ describes the state of maximal von Neumann entropy, in this case $c \in \mathcal{C}$ is said to be an *achromatic perceived color*. Since the condition $\rho(2\mathbf{v}_c) = \rho_0 = Id_2/2$ is equivalent to $v_{c,1} = v_{c,2} = 0$, it follows that the center of the disk $\mathcal{D}_{1/2}$ represents achromatic colors.

3 The addition law of chromatic vectors

This section is mainly devoted to deriving the Einstein-Poincaré addition law for chromatic vectors. As a consequence, this allows us to endow coherently the space of chromatic vectors with the Hilbert metric. We will show in 3.4 that this metric has a psychovisual counterpart.

3.1 Chromaticity descriptors: purities and quantities

For the sake of simplicity, we will consider only colors c whose chromatic vectors are of the form $\mathbf{v}_c = (v_c, 0)$ with $-1/2 \leq v_c \leq 1/2$. The two chromatic vectors $\mathbf{v}_+ = (1/2, 0)$ and $\mathbf{v}_- = (-1/2, 0)$ are *pure opponent* chromatic vectors. Given a color c, its chromatic vector $\mathbf{v}_c$ divides the segment connecting $\mathbf{v}_-$ and $\mathbf{v}_+$ (extremes excluded) in two parts, whose lengths are denoted by $p^-(c)$ and $p^+(c)$, where:

$$p^-(c) = \frac{1}{2} - v_c = \frac{1 - 2v_c}{2} \ , \tag{30}$$

will be called the $-$ *purity* of c and

$$p^+(c) = v_c - \left(-\frac{1}{2}\right) = \frac{1 + 2v_c}{2} \ , \tag{31}$$

will be called the $+$ *purity* of c. The sum of the $-$ and $+$ purity of c is 1, so $\mathbf{v}_c$ can be written as the convex combination of the pure opponent chromatic vectors $\mathbf{v}_-$ and $\mathbf{v}_+$ with weights given by p^- and p^+, respectively, i.e. $\mathbf{v}_c = p^-(c)\mathbf{v}_- + p^+(c)\mathbf{v}_+$.

The term 'purity' is particularly appropriate, not only because it involves the pure opponent chromatic vectors, but also because it is reminiscent of the same term appearing in classical CIE (Commission International de l'Éclairage) colorimetry. Indeed, also the definition of excitation purity p_e of a color c carries the information about its position on a straight line, precisely the one joining the equienergy point w (achromatic color) of the CIE 1931 chromaticity diagram with the so-called dominant wavelength of c (represented by a point belonging to the border of the chromaticity diagram). See [22] for more details.

Let also denote

$$r(c) = \frac{p^-(c)}{p^+(c)} = \frac{1 - 2v_c}{1 + 2v_c} \ , \tag{32}$$

the *purity ratio* of the color c. We have:

$$v_c = \frac{1}{2}\left(\frac{p^+(c) - p^-(c)}{p^+(c) + p^-(c)}\right) \ . \tag{33}$$

It is obvious that, given two colors c and c', we have:

$$\mathbf{v}_c = \mathbf{v}_{c'} \iff p^+(c) = p^+(c') \iff p^-(c) = p^-(c') \ . \tag{34}$$

Two colors with the same purity differ only by their magnitude. For this reason, it is useful to define a color attribute analogue to purity but which takes into account also the magnitude information that has been lost after the projection on $\mathcal{D}_{1/2}$. This is done as follows: we define the $-$ *quantity* of a color c by:

$$q^-(c) = 2\alpha_c p^-(c) = \alpha_c(1 - 2v_c) \ , \tag{35}$$

and similarly the + *quantity* by:

$$q^+(c) = 2\alpha_c p^+(c) = \alpha_c(1 + 2v_c) \ , \tag{36}$$

where α_c is the magnitude of c.

Of course, perceived colors with magnitude equal to 1/2, i.e. color states, are characterized by the fact that their purities and quantities coincide.

3.2 Einstein-Poincaré addition law

Now, we discuss our main issue: *how can we describe a given color c relatively to another given color d*? One intuitive way to do it is to compare $q^-(c)$ with $q^-(d)$ and $q^+(c)$ with $q^+(d)$, that is to compare their − and + *quantities*. For this, we can consider the *quantity ratios*:

$$s^+(c,d) = \frac{q^+(c)}{q^+(d)} \quad \text{and} \quad s^-(c,d) = \frac{q^-(c)}{q^-(d)} \ . \tag{37}$$

If we only know the numerical values of $q^\pm(c)$, $q^\pm(d)$ and not their explicit expressions (35) and (36), then using the quantity ratio to compare c and d makes sense only if d is a color state. In fact, and to take an example, if c and d are two perceived colors with the same chromatic vector, the ratio, for instance, $s^+(c,d)$ does not give any information about the description of c relatively to d since we do not know the magnitude of d.

Let us consider two arbitrary colors c and d whose magnitudes and chromatic vectors are respectively α_c and α_d, and $\mathbf{v}_c$ and $\mathbf{v}_d$, with $v_c > v_d$. We have:

$$s^+(c,d) = \frac{\alpha_c p^+(c)}{\alpha_d p^+(d)} \quad \text{and} \quad s^-(c,d) = \frac{\alpha_c p^-(c)}{\alpha_d p^-(d)} \ . \tag{38}$$

In order to describe c with respect to d, we have to perform quantity ratios between c and d_s, this latter being the color state whose chromatic vector equals $\mathbf{v}_d$. We write:

$$s^+(c,d) = \frac{q^+(c)}{2\alpha_d p^+(d_s)} = \frac{q^+(c)}{2\alpha_d q^+(d_s)} = \frac{1}{2\alpha_d} s^+(c,d_s) \ , \tag{39}$$

and the same with the minus sign.

Now we arrive to the key definition of a chromatic vector, that we will denote with $\mathbf{v}_d^c$, that describes the color c with respect to d. In order to do that, we take inspiration from eq. (33) with quantity ratios playing the role of purities, thus obtaining:

$$v_d^c = \frac{1}{2}\left(\frac{s^+(c,d_s) - s^-(c,d_s)}{s^+(c,d_s) + s^-(c,d_s)}\right) \ . \tag{40}$$

We have:

$$v_d^c = \frac{1}{2}\left(\frac{q^+(c)q^-(d) - q^-(c)q^+(d)}{q^+(c)q^-(d) + q^-(c)q^+(d)}\right) \ , \tag{41}$$

that is:

$$v_d^c = \frac{1}{2}\left(\frac{p^+(c)p^-(d) - p^-(c)p^+(d)}{p^+(c)p^-(d) + p^-(c)p^+(d)}\right) \ . \tag{42}$$

Now we compute:

$$\frac{v_c - v_d}{1 - 4v_c v_d} = \frac{\frac{1}{2}\left(\frac{p^+(c)-p^-(c)}{p^+(c)+p^-(c)}\right) - \frac{1}{2}\left(\frac{p^+(d)-p^-(d)}{p^+(d)+p^-(d)}\right)}{1 - \frac{p^+(c)-p^-(c)}{p^+(c)+p^-(c)} \cdot \frac{p^+(d)-p^-(d)}{p^+(d)+p^-(d)}} \ . \tag{43}$$

We have:

$$\frac{v_c - v_d}{1 - 4v_c v_d} = \frac{1}{2}\left(\frac{(p^+(d)+p^-(d))(p^+(c)-p^-(c)) - (p^+(d)-p^-(d))(p^+(c)+p^-(c))}{(p^+(c)+p^-(c))(p^+(d)+p^-(d)) - (p^+(c)-p^-(c))(p^+(d)-p^-(d))}\right) \tag{44}$$

This shows that:

$$\mathbf{v}_d^c = \frac{\mathbf{v}_c - \mathbf{v}_d}{\mathbf{1} - 4\mathbf{v}_c\mathbf{v}_d} \ , \tag{45}$$

or equivalently:

$$\mathbf{v}_c = \frac{\mathbf{v}_d^c + \mathbf{v}_d}{\mathbf{1} + 4\mathbf{v}_d^c\mathbf{v}_d} \ . \tag{46}$$

This means that chromatic vectors can be considered as the analogue of relativistic velocities. Note that the factor 4 in eq. (46) is due to the fact that chromatic vectors have norms less or equal to 1/2, i.e. that in our model the limiting saturation Σ (or the speed of light in mechanics) is equal to 1/2. It is clear that if $\mathbf{v}_d^c = (\Sigma, 0)$ in eq. (46), then $\mathbf{v}_c = (\Sigma, 0)$, which is precisely the mathematical expression of the result of Yilmaz second experiment.

3.3 Hilbert metric and Einstein-Poincaré addition law

The fact that chromatic vectors verify the addition law given by Eq. (46) allows to express a constancy property in terms of Hilbert distances.

Let us first recall that given four collinear points a, p, q, and b of $\mathbb{R}^2$, the cross ratio $[a, p, q, b]$ is defined by [14]:

$$[a, p, q, b] = \frac{\|q - a\|}{\|p - a\|} \cdot \frac{\|p - b\|}{\|q - b\|} \ , \tag{47}$$

where $\|\cdot\|$ denotes the Euclidean norm. Given two points p and q of the closed disk $\mathcal{D}_{1/2}$ such that the points $(-1/2, 0) = a_-$, p, q, and $(1/2, 0) = a_+$ are collinear, with the segment $[p, q]$ contained in the segment $[a_-, a_+]$, the $\mathcal{D}_{1/2}$-Hilbert distance $d_H(p, q)$ is given by [14]:

$$d_H(p, q) = \frac{1}{2} \ln [a_-, p, q, a_+] \ , \tag{48}$$

where the choice of the points involved in the cross ratio above guarantees that the argument of ln is strictly positive.

We consider now three chromatic vectors $\mathbf{v}_c$, $\mathbf{v}_d$ and $\mathbf{v}_d^c$ of $\mathcal{D}_{1/2}$ with $\mathbf{v}_c = (v_c, 0)$, $\mathbf{v}_d = (v_d, 0)$ and $\mathbf{v}_d^c = (v_d^c, 0)$. We have the following elementary result (see for instance [15] for related topics).

Proposition 3.1 *With the above notations:*

$$d_H((0,0),(v_d^c,0)) = d_H((v_d,0),(v_c,0)) \iff v_c = \frac{v_d^c + v_d}{1 + 4v_d^c v_d} \ . \tag{49}$$

Proof. By definition, the equality $d_H((0,0),(v_d^c,0)) = d_H((v_c,0),(v_d,0))$ holds if and only if $[a_-, (0,0), (v_d^c,0), a_+] = [a_-, (v_d,0), (v_c,0), a_+]$. Equivalently:

$$d_H((0,0),(v_d^c,0)) = d_H((v_c,0),(v_d,0)) \iff \frac{1/2 - v_c}{1/2 + v_c} = \frac{1/2 - v_d^c}{1/2 + v_d^c} \cdot \frac{1/2 - v_d}{1/2 + v_d} \ . \tag{50}$$

By direct computation, it can be checked that this last equation is equivalent to eq. (49). □

The colorimetric interpretation of the relation:

$$d_H(\mathbf{0}, \mathbf{v}_d^c) = d_H(\mathbf{v}_d, \mathbf{v}_c) \iff \mathbf{v}_c = \frac{\mathbf{v}_d^c + \mathbf{v}_d}{1 + 4\mathbf{v}_d^c\mathbf{v}_d} \tag{51}$$

is the following. The vector $\mathbf{v}_d^c$ appears in the relativistic sum equation expressed by (46) together with the chromatic vectors $\mathbf{v}_c$ and $\mathbf{v}_d$ if and only if the Hilbert length $d_H(\mathbf{0}, \mathbf{v}_d^c)$ of $\mathbf{v}_d^c$ is equal to the Hilbert distance between $\mathbf{v}_c$ and $\mathbf{v}_d$. Since $\mathbf{v}_d^c$ describes the color c with respect to the color d, this result implies that the Hilbert distance is a mathematically coherent candidate for a perceptual metric of chromatic attributes.

A geometric representation of this result is provided by the so-called Chasles theorem on cross ratios of cocyclic points, see Fig. 3.3, which provides a graphical method to construct the relativistic sum of two vectors in one dimension. Although elementary, this result reveals a meaningful link between the Einstein-Poincaré addition law of chromatic vectors and the Hilbert metric, which, on $\mathcal{D}_{1/2}$, coincides precisely with the *Klein hyperbolic metric* defined by:

$$ds^2_{\mathcal{D}_{1/2}} = \frac{(1/4 - v_2^2)dv_1^2 + 2v_1v_2dv_1dv_2 + (1/4 - v_1^2)dv_2^2}{(1/4 - \|v\|^2)^2} \ . \tag{52}$$

The geodesics with respect to this metric are straight chords of $\mathcal{D}_{1/2}$.

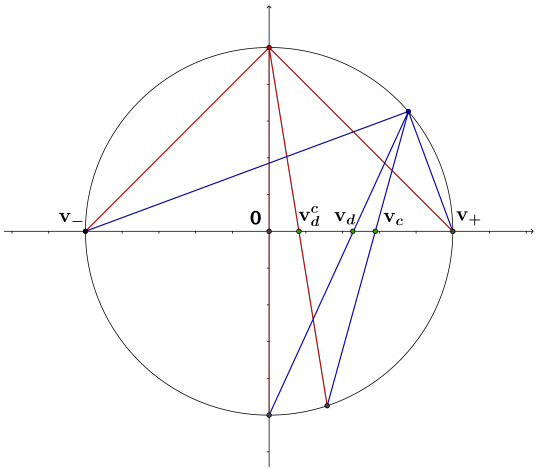

Figure 2: Illustration of the result of Prop. (3.1) by Chasles theorem on the cross ratios of cocyclic points. $\mathbf{v}_c$, $\mathbf{v}_d$ and $\mathbf{v}_d^c$ satisfy eq. (51).

3.4 Compatibility of the Hilbert metric with psycho-physical experimental data

Now we address the important issue of the compatibility between the Hilbert metric on $\mathcal{D}_{1/2}$ and psychovisual measurements. This is not an easy task because of two reasons: firstly, experimental data on color perception are very scarce, secondly, psychovisual measurements are always affected by subjective variations which imply the use of averaging procedures that inevitably reduce the measure accuracy.

The only psychovisual results consistent with our framework that we were able to find are those reported in [16] and [17]. The authors conducted their tests with the help of the standard CIE illuminants C (near-daylight, $(x_C, y_C) = (0.3125, 0.3343)$) and A (tungsten, $(x_A, y_A) = (0.4475, 0.4084)$) and added a third one, denoted with G (greenish, $(x_G, y_G) = (0.3446, 0.4672)$). The values (x, y) represent the CIE xyY chromaticity coordinates of C, A and G, respectively, Fig. 3.4 shows their position in the chromaticity diagram.

In what follows, observers adapted to the illuminants C, A and G, respectively, will be denoted by $o_1 = (c, C)$, $o_2 = (a, A)$ and $o_3 = (g, G)$.

A haploscope is used to compare the color perception of one eye always adapted to the illuminant C and the other eye adapted to C, A and G.

Fig. 3.4 shows, in the xyY diagram, three families of curves obtained by the tests performed in [17]:

1. the first is composed by three contours surrounding C that correspond to color stimuli with fixed Munsell value, different hue but with the same perceived Munsell chroma in $\{2, 4, 8\}$.

By normalizing these data between 0 and 0.5 we obtain $\{0.1, 0.2, 0.4\}$, which are the norms of the chromatic vectors $\mathbf{v}_c^1$ of the colors associated to the corresponding stimuli observed by o_1;

2. the second and the third are given by two contours surrounding A, resp. G, that correspond to colors c with varying hues and whose Munsell chroma belong to the set $\{2, 4\}$. The chromatic vectors $\mathbf{v}_c^2$, resp. $\mathbf{v}_c^3$, of these colors observed from o_2, resp. o_3, have norms belonging to the set $\{0.1, 0.2\}$.

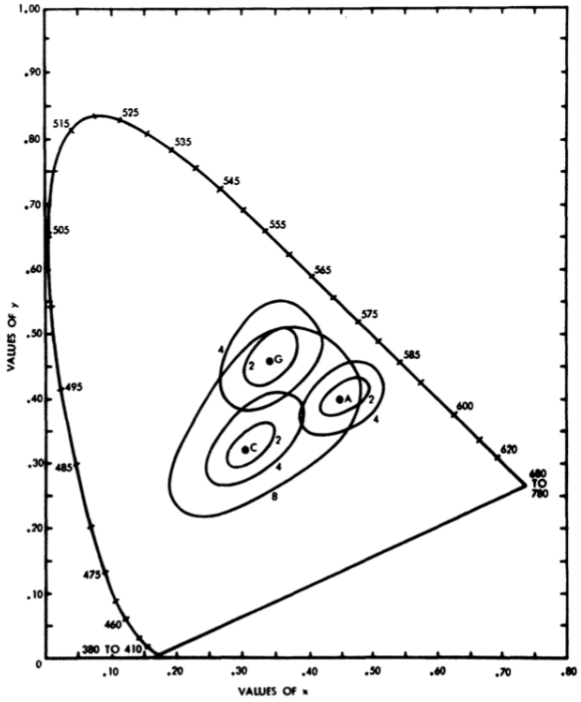

Figure 3: The iso Munsell chroma contours found by [17] in the xyY diagram.

As discussed above, the psychovisual data reported in [16] and [17] are only averaged, thus, the only kind of information that we have from Fig. 3.4 is, for example, that the xyY coordinates of standard illuminant A are between the curves of chroma 4 and 8 of the observer o_1. Thus, the norm of the chromatic vectors is not possible to achieve with accuracy. However, in order to test our mathematical theory, as a first approximation, we perform a linear interpolation from the data appearing in the figure, which gives $\|\mathbf{v}_a^1\| \simeq 6.76/20 = 0.338$.

In Fig. 4(a), we denote by F and F' the xyY coordinates of the points in the xyY diagram obtained by the intersection between the line connecting A and C with the iso-chroma contours for o_1 and o_2, respectively.

The color F is perceived by o_1 as having a chromatic vector $\mathbf{v}_f^1$ with norm $\|\mathbf{v}_f^1\| = 0.2$. By construction, we determine F', the color perceived by o_2 with chromatic vector $\mathbf{v}_{f'}^2$ such that $\mathbf{v}_{f'}^2 = \mathbf{v}_f^1$. Again, by linear interpolation, the norm of the chromatic vector $\mathbf{v}_{f'}^1$ corresponding to the color F' perceived by o_1, is approximated by $\|\mathbf{v}_{f'}^1\| \simeq 3.76/20 = 0.188$. Fig. 4(b) shows all the chromatic vectors in the disk $\mathcal{D}_{1/2}$.

One can easily check, as illustrated by Chasles theorem, that:

$$d_H(\mathbf{v}_f^1, \mathbf{v}_c^1) = d_H(\mathbf{v}_{f'}^2, \mathbf{v}_a^2) = d_H(\mathbf{v}_{f'}^1, \mathbf{v}_a^1) \ . \tag{53}$$

The same reasoning applied to the situation depicted in Fig. 5(a), where the points $F2$ and

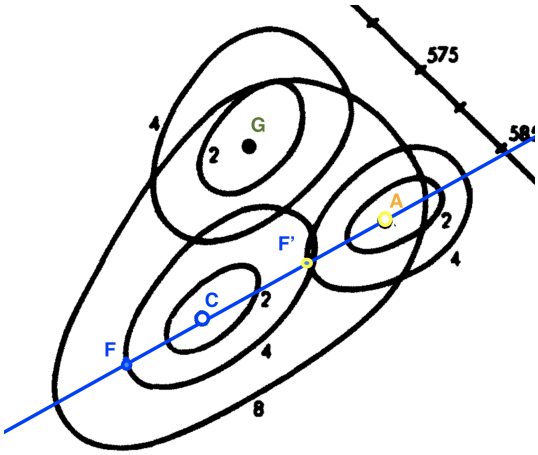

(a) The illuminants C and A and the colors F and F' in the xyY diagram.

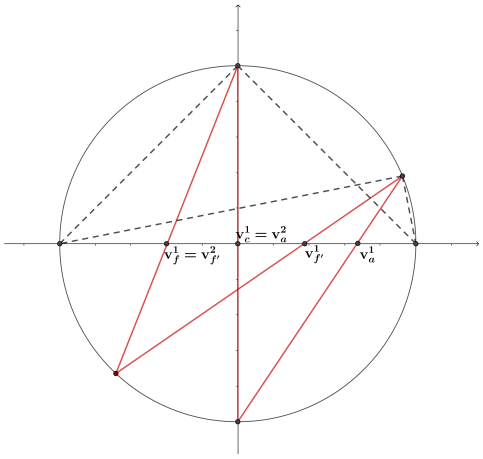

(b) Illustration of the equalities of eq. (53) in the disk $\mathcal{D}_{1/2}$.

Figure 4: Invariance of the Hilbert distance under observer changes: illuminants C and A, and colors F and F'.

$F2'$ belong to another iso-chroma contour, leads to:

$$d_H(\mathbf{v}_{f2}^1, \mathbf{v}_c^1) = d_H(\mathbf{v}_{f2'}^2, \mathbf{v}_a^2) = d_H(\mathbf{v}_{f2'}^1, \mathbf{v}_a^1) \ , \tag{54}$$

see Fig. 5(b).

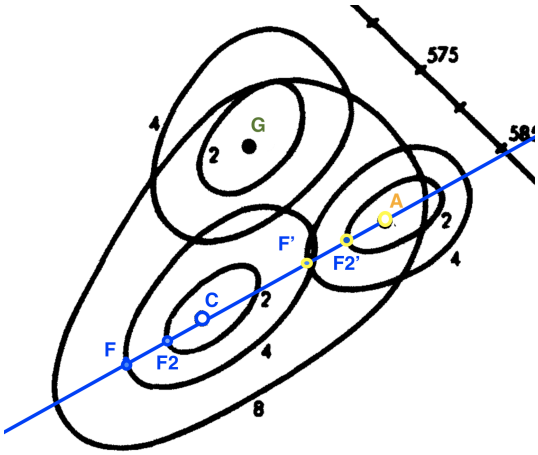

(a) The illuminants C and A and the colors F and F', and $F2$ and $F2'$ in the CIE xyY diagram.

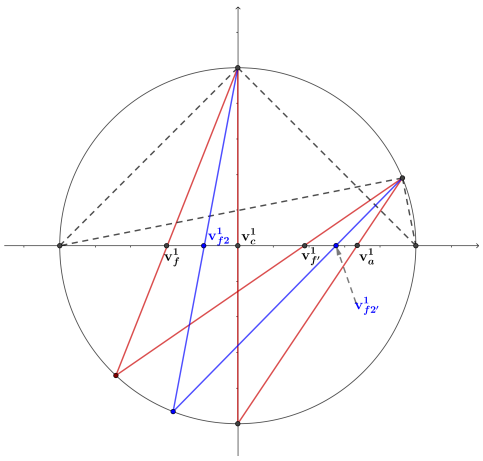

(b) Illustration of the equalities of Eq. (54) in the disk $\mathcal{D}_{1/2}$.

Figure 5: Invariance of the Hilbert distance under observer changes: illuminants C and A, and colors F, F', $F2$, and $F2'$.

Finally, we consider the quite more complicated situation depicted in Fig. 6(a). It is precised in [16] that '*A change from a blue (C) adaptation to a yellow (A) adaptation shows vectors running in a blue-yellow direction, a change from a blue (C) adaptation to a green (G) adaptation shows vectors running in a blue-green direction.*' This means that the angle between $\mathbf{v}_a^1$ and $\mathbf{v}_g^1$ is equal to $\pi/4$.

From Fig. 6(a) we can approximate the norm of the chromatic vector $\mathbf{v}_g^1$: $\|\mathbf{v}_g^1\| \simeq 0.32$. The chromatic vectors $\mathbf{v}_h^1$ and $\mathbf{v}_{h''}^3$ of the two colors H and H'' marked on Fig. 6(a) are equal. Once again, one can easily check that:

$$d_H(\mathbf{v}_h^1, \mathbf{v}_c^1) = d_H(\mathbf{v}_{h''}^3, \mathbf{v}_g^3) = d_H(\mathbf{v}_{h''}^1, \mathbf{v}_g^1) \ , \tag{55}$$

see Fig. 6(b).

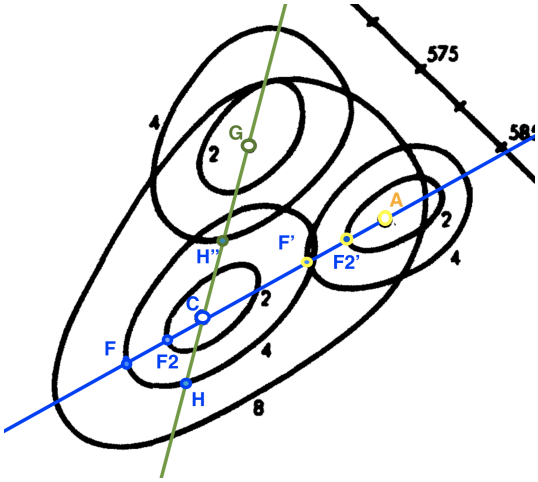

(a) The three illuminants C, A and G, and the colors F and F', $F2$ and $F2'$, and H and H'' in the xyY diagram.

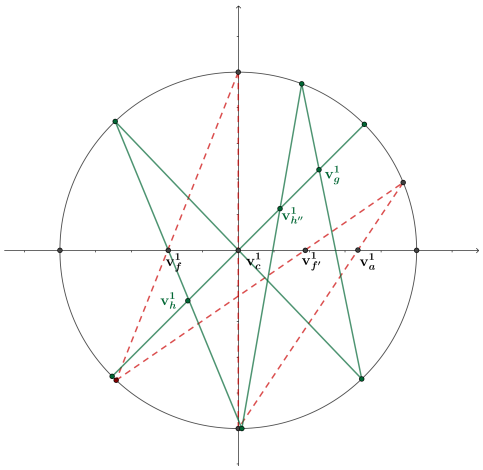

(b) Illustration of the equalities of Eq. (55) in the disk $\mathcal{D}_{1/2}$.

Figure 6: Invariance of the Hilbert distance under observer changes: illuminants C and G, and colors H and H'', compared with illuminants C and A, and colors F and F'.

These discussions show clearly that the Hilbert metric is compatible with the only psychovisual data that we have at disposal. Here we have reported only three cases, but other three configurations related to Fig. 3.4 can be studied and our computations showed that they give rise to the same conclusions.

We have only treated the case when colors, e.g. F and F', have chromatic vectors collinear to the new observer chromatic vector, e.g. $\mathbf{v}_f^1$ and $\mathbf{v}_{f'}^1$ are collinear to $\mathbf{v}_a^1$ in this first situation. Dealing with arbitrary colors needs the introduction of more sophisticated mathematical tools to take into account the general addition law for non-collinear vectors. We prefer to not enter in such details in the present work and to postpone the general case for future research.

4 Chromatic states and boost maps

In order to recover the colorimetric aberration effect from the trichromacy axiom, we explain how pure chromatic states generate Lorentz boost maps and study the action of these boost maps on the space of chromatic vectors.

4.1 One parameter subgroups of boost maps

Let us recall that the pure chromatic states are given by density matrices of the form:

$$\rho(\mathbf{v}) = \frac{1}{2}(Id_2 + \mathbf{v}\cdot\sigma) = \frac{1}{2}\begin{pmatrix} 1+v_1 & v_2 \\ v_2 & 1-v_1 \end{pmatrix} \ , \tag{56}$$

where $\mathbf{v} = (v_1, v_2)$ is a unit vector of $\mathbb{R}^2$. We have the following result.

Proposition 4.1 *Every pure chromatic state generates a one-parameter subgroup of Lorentz boosts [7].*

Proof. The matrix

$$A(\mathbf{v},\zeta_0)=\exp\left(\zeta\frac{\mathbf{v}\cdot\sigma}{2}\right)\ , \tag{57}$$

with ζ_0 a real parameter, is an element of the group $PSL(2,\mathbb{R})$. Using the action of $PSL(2,\mathbb{R})$ on $\mathcal{H}(2,\mathbb{R})$ we can consider the matrices given by:

$$\sigma_i\longmapsto A(\mathbf{v},\zeta_0)\sigma_i A(\mathbf{v},\zeta_0)\ , \tag{58}$$

for $i=0,1,2$ with $\sigma_0=Id_2$. The matrix with entries

$$M(\mathbf{v},\zeta_0)_{ij}=\frac{1}{2}\mathrm{Trace}\left(\sigma_i A(\mathbf{v},\zeta_0)\sigma_j A(\mathbf{v},\zeta_0)\right)\ , \tag{59}$$

is the matrix

$$M(\zeta)=\begin{pmatrix}\cosh(\zeta_0) & v_1\sinh(\zeta_0) & v_2\sinh(\zeta_0)\\ v_1\sinh(\zeta_0) & 1+v_1^2(\cosh(\zeta_0)-1) & v_1v_2(\cosh(\zeta_0)-1)\\ v_2\sinh(\zeta_0) & v_1v_2(\cosh(\zeta_0)-1) & 1+v_2^2(\cosh(\zeta_0)-1)\end{pmatrix}\ , \tag{60}$$

with $\zeta=\tanh(\zeta_0)(v_1,v_2)$. □

For instance, if $\mathbf{v}=(1,0)$ then:

$$M(\zeta)=\begin{pmatrix}\cosh(\zeta_0) & \sinh(\zeta_0) & 0\\ \sinh(\zeta_0) & \cosh(\zeta_0) & 0\\ 0 & 0 & 1\end{pmatrix}\ . \tag{61}$$

One can easily check that, in this case, the pure chromatic vector $(\cos\theta,\sin\theta)/2$ is sent to the pure chromatic vector $\mathbf{w}=(w_1,w_2)$ with:

$$\begin{cases}2w_1=\dfrac{\tanh(\zeta_0)+\cos\theta}{1+\tanh(\zeta_0)\cos\theta}\\ 2w_2=\dfrac{(1-\tanh(\zeta_0)^2)^{1/2}\sin\theta}{1+\tanh(\zeta_0)\cos\theta}\ .\end{cases} \tag{62}$$

4.2 On Yilmaz's third experiment [5]

The dynamics given by eq. (62) is nothing else than the dynamics of the relativistic aberration effect. It allows, as already suggested by Yilmaz, to explain the results of the third experiment described in [5].

The pure chromatic vector $(0,1)/2$ is sent to the pure chromatic vector with coordinates $(\tanh(\zeta_0),(1-\tanh(\zeta_0)^2)^{1/2})/2$ whereas the pure chromatic vector $(1,0)/2$ remains unchanged. When the rapidity ζ_0 increases, $\tanh(\zeta_0)$ approaches 1 and the vector $(\tanh(\zeta_0),(1-\tanh(\zeta_0)^2)^{1/2})/2$ approaches the vector $(1,0)/2$. At the limit $\tanh(\zeta_0)=1$, every pure chromatic vector $(\cos\theta,\sin\theta)/2$ is sent to the vector $(1,0)/2$, except the vector $(-1,0)/2$.

This means that every pure chromatic vector, except the green pure chromatic vector, can be transformed to a pure chromatic vector arbitrarily close to the red pure chromatic vector under the Lorentz boost of eq. (61) if the rapidity ζ_0 is sufficiently great. To explain the results of Yilmaz third experiment in view of eq. (62), note that w_1 is the cosine of the angle of the ray from the achromatic vector to the image of the chromatic vector $(\cos\theta,\sin\theta)/2$ viewed under the initial illuminant I, whereas

$$\overline{w}_1=\frac{-\tanh(\zeta_0)+\cos\theta}{1-\tanh(\zeta_0)\cos\theta} \tag{63}$$

is the cosine of the angle of the ray from the achromatic vector to the image of the chromatic vector $(\cos\theta,\sin\theta)/2$ viewed under the illuminant I'. In consequence, under the illuminant I', the expected yellow chromatic vector given by $\theta=\pi/2$ is in fact the greenish chromatic vector given by $\cos\theta=-\tanh(\zeta_0)$.

5 Conclusion

At the end of this study, it clearly appears that the best way to report psychovisual experiments of color matching type is to consider chromatic vector transformations. The space of chromatic vectors is the disk $\mathcal{D}_{1/2}$. We have shown that this space is a colorimetric analogue of the special relativity space of velocities. It is endowed with the Riemannian hyperbolic Klein metric. Reports on experiments using real data have proven the soundness of our proposal. Moreover, we have explained that this approach, which relies on the sole trichromacy axiom, also takes into account color opponency from a quantum point of view. This means that color perception is a kind of quantum relativistic phenomenon in which hyperbolicity plays a crucial role. The mathematical and rigorous model that we have described seems to be a very relevant alternative to the model commonly used in colorimetry.

We are currently investigating the mathematical details of the extension of our proposal from collinear chromatic vectors to the general case in which chromatic vectors do not necessarily lie on the same axis.

We also consider interesting to study how the novel objects and formalism that we have introduced in this work can be used in practice for colorimetric purposes and how they relate to existing color spaces represented in cylindrical coordinates such as the HSV space.

To this aim, and also to more finely test our proposal, it is paramount to complement the exiguous psychovisual data that we currently have at disposal and possibly to design new kind of experiments.

6 Appendix - Description of Yilmaz experiments

The generic apparatus for the experiments is shown in Fig. 7, where we can see two identical rooms R_1 and R_2, separated by a common wall with a thin hole and illuminated by the sources of light S_1 and S_2. Both rooms are painted with a non-selective Lambertian white paint. A piece of white paper is divided in two parts and they are placed in the rooms, so that an observer can perceive them simultaneously. The key point is that one piece is seen directly and the other through the hole.

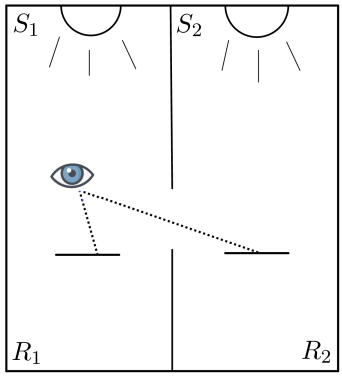

Figure 7: The experimental apparatus considered by Yilmaz.

The illumination S_1 of room R_1 will always be provided by near-daylight broadband illuminants. Instead, the illumination of room R_2 will be provided by a light source S_2 that can also be narrow-band. The perceived colors are compared with the help of a set of Munsell chips enlighted by the same illuminant under which the observer is adapted.

In order for the reader to make up his or her own mind about the interpretation and feasibility of the experiments, we quote Yilmaz [5].

6.1 The first experiment

'*If the sources S_1 and S_2 are chosen to be two different illuminants of near-daylight chromaticity, I and I', then the wall of each room is perceived as white by the observer in the room but the wall of the other room, as seen through the hole, appears chromatically colored. Furthermore, if R_2 appears with the saturation σ from R_1, then R_1 appears with the saturation approximately $-\sigma$ from R_2, the minus sign indicating that the hue is complementary to the former hue.*'

6.2 The second experiment

'*If S_2 is chosen to be a single-frequency source, say, that corresponding to the long-wave (red) extreme of the visible spectrum $\overline{R}$, then the saturation Σ observed through the hole (observer being in R_1) is too high to be duplicated by any of the Munsell chips, and remains practically the same if we change the illuminant from I to I' in R_1.*'

6.3 The third experiment

'*Let S_2 be a source of frequency corresponding to the yellow part of the spectrum, $\overline{Y}$, separated in the hue circle by 90 degrees from spectrum red, $\overline{R}$. Then if we change the illuminant in R_1 from I to I', the hue of $\overline{Y}$ is seen to change by an amount φ such that $\sin\varphi \simeq \sigma/\Sigma$. No variation seems to take place in its saturation.*'

References

[1] I. Newton, *Opticks, or, a treatise of the reflections, refractions, inflections & colours of light.* Courier Corporation, 1952.

[2] H. Grassmann, *Zur theorie der farbenmischung.* Annalen der Physik, 165(5):69–84, 1853.

[3] B. Riemann, *Über die hypothesen, welche der geometric zu grunde liegen. In* The Collected Works of Bernhard Riemann. Dover Books on Mathematics, New York, 2017.

[4] E. Schrödinger, *Grundlinien einer theorie der farbenmetrik im tagessehen (Outline of a theory of colour measurement for daylight vision).* Available in English in Sources of Colour Science, Ed. David L. Macadam, The MIT Press (1970), 134-82. *Annalen der Physik*, 63(4):397–456; 481–520, 1920.

[5] H. Yilmaz, *On color perception.* Bulletin of Mathematical Biophysics, 24, 5-29, 1962.

[6] N. D. Mermin, *Relativity without light.* American Journal of Physics 52, 119, 1984.

[7] M. Berthier, *Geometry of color perception. Part 2: perceived colors from real quantum states and Hering's rebit.* Submitted to the Journal of Mathematical Neuroscience. Preprint available at: https://hal.archives-ouvertes.fr/hal-02342456/document.

[8] M. Berthier and E. Provenzi, *From Riemannian trichromacy to quantum color opponency via hyperbolicity.* Submitted to the Journal of Mathematical Imaging and Vision. Preprint available at: https://hal.archives-ouvertes.fr/hal-02479897/document.

[9] E. Provenzi, *Geometry of color perception. Part 1: Structures and metrics of a homogeneous color space.* Submitted to the Journal of Mathematical Neuroscience. Preprint available at: https://hal.archives-ouvertes.fr/hal-02336556/document.

[10] H. L. Resnikoff, *Differential geometry and color perception.* Journal of Math. Biology, 1, 97-131, 1974.

[11] J. C. Baez, *Division algebras and quantum theory.* Foundations of Physics, 42(7):819–855, 2012.

[12] S. K. Shevell and P. R. Martin, *Color opponency: tutorial*. J Opt Soc Am A Opt Image Sci Vis. 34(7): 1099-1108, 2017.

[13] F. A. A. Kingdom, *Lightness, brightness and transparency: A quarter century of new ideas, captivating demonstrations and unrelenting controversy*. Vision Research 51, 652–673, 2011.

[14] B. Colbois and C. Vernicos, *Les géométries de Hilbert sont à géométrie bornée*. Ann. Inst. Fourier, 57, 4, 1359-1375, 2007.

[15] V. Fock, *The theory of space, time, and gravitation*. Pergamon Press LTD, 1959.

[16] R. W. Burnham, R. M. Evans, and S. M. Newhall, *Prediction of color appearance with different adaptation illuminations*. JOSA, 47, 1, 35-42, 1957.

[17] C. P. Crocetti and W. P. Bethke, *Application of color vision to two-color mixtures, Final Report*. Scientific and Technical Aerospace Reports, Vol. 1, 20, N63-20301, 1963. Available at: https://apps.dtic.mil/dtic/tr/fulltext/u2/414822.pdf.

[18] A. Gilchrist, C. Kossyfidis, F. Bonato, T. Agostini, J. Cataliotti, X. Li, B. Spehar, V. Annan and E. Economou, *An anchoring theory of lightness perception*. Psychological review, 106(4), p.795.

[19] L. D. Landau and E. M. Lifshitz, *Classical field theory*, Course of Theoretical Physics vol 2, 1975.

[20] K. Lechner, *Classical Electrodynamics: A Modern Perspective*, Springer Nature, 2018.

[21] M. D. Fairchild, *Color appearance models*, John Wiley & Sons, (2013).

[22] G. Wyszecky and W. S. Stiles, *Color science*, Wiley, (1982).